Strategies for laser-induced fluorescence detection of nitric oxide in high-pressure flames. I. *A–X*(0,0) excitation

Wolfgang G. Bessler, Christof Schulz, Tonghun Lee, Jay B. Jeffries, and Ronald K. Hanson

Three different high-pressure flame measurement strategies for NO laser-induced fluorescence (LIF) with *A–X*(0,0) excitation have been studied previously with computational simulations and experiments in flames up to 15 bars. Interference from O_2 LIF is a significant problem in lean flames for NO LIF measurements, and pressure broadening and quenching lead to increased interference with increased pressure. We investigate the NO LIF signal strength, interference by hot molecular oxygen, and temperature dependence of the three previous schemes and for two newly chosen excitation schemes with wavelength-resolved LIF measurements in premixed methane and air flames at pressures between 1 and 60 bars and a range of fuel/air ratios. In slightly lean flames with an equivalence ratio of 0.83 at 60 bars, the contribution of O_2 LIF to the NO LIF signal varies between 8% and 29% for the previous schemes. The O_2 interference is best suppressed with excitation at 226.03 nm. © 2002 Optical Society of America

OCIS codes: 300.2530, 280.1740, 280.2470.

1. Introduction

Detection of nitric oxide during combustion is of particular interest as NO is one of the most important combustion-generated pollutants. Automotive engines and gas turbines play a major role in the overall production of NO, which influences atmospheric ozone depletion and smog formation. In the future, drastic regulatory restrictions on NO release are expected. Despite use of catalytic converters for NO abatement, it is an important task to make engine exhaust cleaner. Imaging measurements during the formation of the pollutant within the combustion process have attracted much interest to aid the development of simulation models and to provide a tool for the optimization of practical combustion systems. Many of these practical devices operate at elevated pressures, and a strategy for quantitative laser-induced fluorescence (LIF) imaging of NO at pressures in excess of 50 bars is desired.

LIF can provide instantaneous two-dimensional images of absolute concentration fields without perturbing the process under investigation.[1,2] Several studies have addressed NO imaging measurements in practical combustion processes such as high-pressure burners and gasoline and Diesel internal combustion engines.[3–8] In further experiments, NO LIF imaging was used for temperature measurements[9–11] and flow visualization.[12]

Different approaches for NO excitation have been previously suggested, including NO excitation in the *D–X*(0,1) band and several *A–X* vibrational bands. The literature does not give clear guidelines as to which transitions are favorable in a given diagnostic situation. We examined NO LIF excitation and detection strategies in premixed methane and air flames as a function of an equivalence ratio and pressures between 1 and 60 bars. Wavelength-dispersed LIF spectra are recorded versus excitation wavelength to select the optimum excitation features and fluorescence collection bandpass. Interference LIF is quantified for each of the strategies studied. In a series of papers, we will compare transitions in the *A–X* band and recommend the most appropriate excitation and detection strategies for high-pressure

W. G. Bessler and C. Schulz are with the Physikalisch-Chemisches Institut, Ruprecht-Karls-Universität Heidelberg, Im Neuenheimer Feld 253, 69120 Heidelberg, Germany. T. Lee, J. B. Jeffries (jeffries@navier.stanford.edu), and R. K. Hanson are with the Department of Mechanical Engineering, High Temperature Gasdynamics Laboratory, Stanford University, Stanford, California 94305-3032.

Received 25 September 2001; revised manuscript received 31 January 2002.

0003-6935/02/183547-11$15.00/0

NO LIF. Here we examine excitation of five different regions of the NO A–X(0,0) band and determine the degree of interference LIF.

2. Problems

A. Transmission Properties

Electronic excitation of NO from sufficiently populated states requires short UV wavelengths around 193 nm in the D–X(0,1) band or at 226, 237, 248 nm for excitation in the A–X(0,0), (0,1), and (0,2) bands, respectively. In many high-pressure combustion systems, laser and signal attenuation have been reported to be major problems. Recent experiments showed that hot CO_2 and H_2O are the main contributors to absorption in this spectral range.[13] These compounds exhibit broadband absorption behavior with cross sections increasing with temperature and decreasing with wavelength.[14] This effect increases with pressure because of the increasing number density of absorbers.

Transmission properties therefore limit the NO detection strategy choice [3,15] and often rule out the application of D–X excitation in the presence of hot combustion products at high pressures. Most experiments therefore focus on the A–X system using various detection strategies, exciting different rotational transitions in the (0,0) band as well as transitions in the (0,1) and (0,2) bands, which further reduce laser attenuation.

B. O_2 Laser-Induced Fluorescence Interference

The main concern when we choose a potential wavelength for NO excitation is the suppression of spectral overlap of excitation of other species that might result in an interfering LIF signal. Hot O_2 is the main contributor to LIF interference in lean and nonpremixed flames. The Schumann–Runge bands of O_2 overlap with the NO gamma bands [16] over a wide range of excitation wavelengths resulting in the O_2 fluorescence signal overlapping with NO LIF. Measurements with spectrally resolved detection of the fluorescence light provide a way to distinguish between different signal contributions on the basis of their spectral signature. However, this approach is generally limited to zero- or one-dimensional measurements. For imaging measurements, bandpass filters are typically not suited to separate the overlapping signal intensities.

The ratio of O_2 LIF background increases with pressure for two reasons: variation in fluorescence quantum yield and variation in spectral overlap with the laser profile because of line broadening:

(i) The effective fluorescence lifetime of NO decreases linearly with pressure because of collisional quenching,[17] whereas the effective fluorescence lifetime of excited O_2 is limited by its fast predissociation[18] and is thus mostly pressure independent.[19] Hence the relative fluorescence quantum yield and therefore the ratio of the O_2 and NO LIF signals increases with pressure.

(ii) As the pressure increases, the spectra are significantly altered by broadening and shifting.[20–22] This increases the spectral overlap between NO and O_2 excitation, making the choice of excitation wavelengths more critical at high pressure. The line broadening also results in reduced spectral overlap of laser lines with the absorption features, which reduces the signal strengths. NO is much more affected by line broadening than O_2, again because of the fast predissociation of O_2. Therefore, with increasing pressure, the ratio of O_2 and NO LIF signals further increases.

C. Interference in Rich Flames

In rich and nonpremixed flames additional signal interference has been observed.[8,23] Broadband fluorescence has been observed that is usually attributed to polycyclic aromatic hydrocarbons and partially burned hydrocarbons (aldehydes, ketones). This signal appears almost exclusively red shifted in respect to the laser wavelength. To avoid its detection, NO excitation from hot vibrational states, e.g., the (0,1) or (0,2) bands with subsequent detection of the blue-shifted NO fluorescence, has been suggested.[8,24] In sooting flames at high laser energies, interference by LIF of laser-generated C_2 has also been reported. Its signal appears both red and blue shifted relative to the excitation laser[25] and must be considered as an additional source of interference.

3. Background

In this paper and the following discussion we focus on the NO A–X(0,0) system at 224–227 nm only. Different strategies have been successfully used for NO measurements in premixed methane and air flames,[26] heptane spray flames,[4] and in internal combustion engines fueled with propane,[6] low-sooting Diesel fuel,[5] and commercial Diesel fuel.[27] To minimize O_2 LIF interference, various transitions have been selected from simulation calculations of NO and O_2 LIF spectra [6,28] and from measured spectra and their dependence on pressure, temperature, and equivalence ratio.[28–31]

Cooper and Laurendeau,[4] Reisel and Laurendeau,[32] and Charlston-Goch et al.[33] used the $Q_2(26.5)$ transition at 225.58 nm for various high-pressure applications after spectroscopic investigations in the 1–15-bar range.[30,31] Dec and Canaan[5] and van den Boom *et al.*[27] used the $P_1(23.5)$, $Q_1 + P_{21}(14.5)$, $Q_2 + R_{12}(20.5)$ feature at 226.03 nm for their in-cylinder Diesel engine measurements. This transition had been proposed earlier by Battles and Hanson[28] on the basis of detailed spectroscopic investigations and studied in flames up to 10 bars by DiRosa *et al.*[29] Bräumer and colleagues chose the $R_1 + Q_{21}(21.5)$ transition at 225.25 nm for their in-cylinder measurements based on simulation calculations.[6]

Different strategies have been proposed for the assessment and correction of remaining O_2 LIF interference. Battles and Hanson,[28] DiRosa *et al.,*[29] and Thomson and colleagues[31] suggested an O_2 background correction based on the subtraction of an ad-

Table 1. Investigated Transitions

Candidate	Transition	Excitation Wavelength	Ground-State Energy ε/k (K)	Reference
High T	$R_1 + Q_{21}(26.5)$, $Q_2 + R_{12}(34.5)$, $P_1(40.5)$	224.82	1750–4032	This paper
Sick	$R_1 + Q_{21}(21.5)$	225.25	1161	6
Laurendeau	$Q_2(26.5)$	225.58	1967	30
DiRosa	$P_1(23.5)$, $Q_1 + P_{21}(14.5)$, $Q_2 + R_{12}(20.5)$	226.03	540–1381	28, 29
Low T	$P_2 + Q_{12}(1.5–4.5)$	226.87	178–232	This paper

ditional LIF measurement off the NO resonance. Both groups suggested off-resonance excitation wavelengths close to the resonant NO line. At pressures >20 bars however, the NO spectra become so dense that a nonresonant excitation within the (0,0) band cannot be found (compare with Fig. 3). Dec and Canaan [5] instead used an off-resonance wavelength of 227.503 that is far off the (0,0) band head at 227.01 nm to demonstrate that O_2 fluorescence was not interfering in their measurements. Furthermore, because O_2 LIF intensities are also strongly wavelength and pressure dependent, it cannot be assured that a measurement at a NO off-resonant position yields correct background intensities.

A different approach termed two-zone detection was proposed by DiRosa *et al.*[29] Here, the signal from O_2 in a second spectral region exclusive of NO provides an indirect measure of the O_2 interference in the NO detection bandpass. To our knowledge, application of this method has not yet been shown. Furthermore, in the 310–400-nm wavelength range, they suggest that, for O_2 polycyclic background detection, strong LIF interference from partially burned combustion intermediates (Polycyclic aromatic hydrocarbons, aldehydes, ketones) must be expected in practical combustion situations.

In addition to the need for minimizing O_2 LIF interference, different authors applied different criteria for the choice of excitation transition. Although Laurendau and colleagues[30–32] chose a line with minimized temperature sensitivity at combustion temperatures, Bräumer *et al.*'s choice was limited by the available laser source; the 248-nm output of a KrF excimer laser is shifted to its first anti-Stokes wavelength at 226 nm in a 10-bar hydrogen cell to give sufficient laser energy (several millijoules) for imaging measurements.[6] The tuning range of the excimer laser, however, limits the choice to rotational states with high ground-state energies.[34] Dec and Canaan used a frequency-doubled optical parametric oscillator system,[5] which could access the full (0,0) spectrum and provides high laser energies for imaging measurements. Cooper and Laurendeau's frequency-doubled dye laser system also provided broad wavelength tuning with sufficient laser energy because they performed only point measurements.[4]

In the present study we compare the different NO A–X(0,0) excitation strategies in spectrally resolved LIF measurements in premixed methane and air flames with different air/fuel ratios in the 1–60-bar range. The candidate transitions are summarized in Table 1. In addition to the three transitions mentioned above, two new transitions with minimized O_2 interference are investigated. These transitions were chosen to cover a large range of ground-state energies for use in a two-line or multiline technique for measurement of rotational temperatures. One of these transitions is within the tuning range of a Raman-shifted KrF excimer laser, providing an alternative choice when we use that laser system.

For the first time to our knowledge, comparisons of the candidates are made under well-defined conditions in terms of relative O_2 interference in lean and stoichiometric flames as a function of pressure and equivalence ratio. In addition, we compare signal strength and temperature dependence. Significant differences lead to the result that one of the candidates is clearly superior to the others. Fluorescence quenching and energy transfer processes are not discussed here. In earlier experiments no dependence of these processes on rotational quantum numbers was found.[35] Although playing an important role for quantitative evaluation of the NO LIF data, these processes can be omitted in this relative comparison.

Whereas this paper focuses on A–X(0,0), a similar comparison of promising transitions within the A–X(0,1) band is nearly completed.[36] The comparison between transitions of different vibrational states including the influence of broadband interference in rich flames in under way.[37]

4. Experiment

Laminar, premixed methane and air flat flames at pressures from 1 to 60 bars were stabilized on a porous, sintered stainless-steel plate of 8 mm in diameter; this burner was mounted in a stainless-steel housing with an inner diameter of 60 mm with pressure stabilization ±0.1 bar.[38] Investigations were performed for fuel/air equivalence ratios of $\phi = 0.83$, 0.93, 1.03, and 1.14. All measurements were carried out with 300 parts per million NO seeded to the feedstock gases to mimic enginelike conditions. Optical access to the flame was possible by way of four quartz windows (Fig. 1).

Laser light (2 mJ at 224–227 nm, 0.4 cm^{-1} FWHM) from a Nd:YAG-pumped (Quanta Ray GCR250) frequency-doubled (β-barium borate) dye laser (LAS, LDL205) was aligned parallel to the burner surface and passed through the center of the flame 2 mm above the burner matrix. The pulse energy was

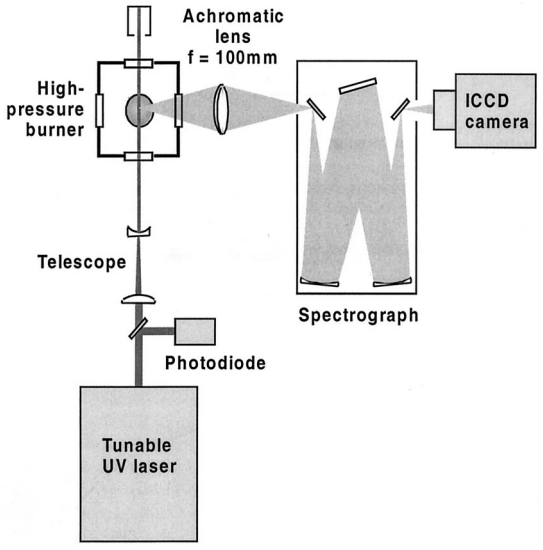

Fig. 1. Experimental arrangement. ICCD, Intensified Charge-coupled device.

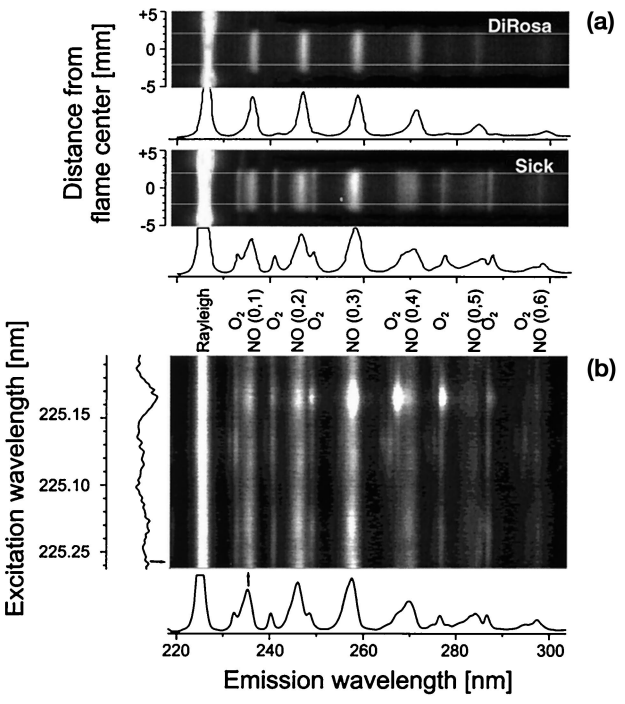

Fig. 2. Construction of an excitation fluorescence chart from measured spectra (a) CCD acquisition of fluoresence intensity versus position along the laser beam with the laser wavelength-tuned resonant with excitation of DiRosa (upper) and Sick (lower) transitions (mditp = 60 bar, $\phi = 0.83$). The center core of the premixed flame (marked by two lines) is averaged over the spatial axis, and the resulting fluorescence spectrum is plotted below each image. Note that the interference of simultaneous O_2 LIF is evident for the Sick excitation. These spectra become the appropriate excitation wavelength in the excitation fluorescence charts (b). (b) Excitation fluorescence chart for a spectral range near the Sick transition for the $p = 40$ bar, $\phi = 0.83$ flame. The arrow in the excitation spectrum indicates the position of the $R_1 + Q_{21}(21.5)$ Sick transition where the emission spectrum was extracted. The arrow in the emission spectrum indicates the NO A–X(0,1) emission where the excitation spectrum was extracted.

measured with a fast photodiode (La Vision). The beam was focused with a cylindrical lens to form a horizontal light sheet with a 3 mm $\times$ 0.5 mm cross section. Fluorescence signals were collected at right angles to the laser beam and focused with a $f =$ 105-mm, $f/4.5$ achromatic UV lens (Nikon) onto the horizontal entrance slit of a 250-mm imaging spectrometer (Chromex 250IS) equipped with a 600-grooves/mm grating. The dispersed fluorescence signals were detected with an intensified CCD camera (LaVision FlameStar III). Each laser pulse yielded a complete fluorescence spectrum maintaining one-dimensional spatial resolution along the laser light path.

The laser was tuned to record excitation spectra around the five candidate transitions, each scan covering ± 0.013 nm in steps of 0.001 nm. The signal was averaged over 20 laser pulses for each excitation wavelength and stored for further evaluation before the laser was scanned to the next wavelength. The 20-shot averaged spectra were corrected for variations in laser-pulse energy.

5. Results and Discussion

We present the results for the investigation of the five candidate transitions within the A–$X(0,0)$ band. For clarity, the transitions used in the literature are hereafter assigned the names Sick, Laurendeau, and DiRosa as defined in Table 1; having in mind a possible application for thermometry, the two new transitions starting from levels with low and high ground-state rotational energies are called low T and high T, respectively.

The camera initially detects images with the spatial resolution along the horizontal path of the laser beam through the flame on one axis and spectral resolution showing emission spectra on the second axis. Two of these images are shown in Fig. 2(a) for typical situations in a lean 60-bar flame with DiRosa and Sick excitation, respectively. The central area of the flame, where temperature and concentrations are homogeneous, is then chosen (marked by the lines in Fig. 2) and integrated over the spatial axis producing the resolved fluorescence spectrum shown in Fig. 2. Each of these spectra becomes a single line in the two-dimensional excitation fluorescence chart shown in Fig. 2(b). After we scan the excitation laser on wavelength the next line is recorded and added to the two-diomensional chart. The resulting two-dimensional excitation and emission charts show excitation and fluorescence wavelengths on the opposite axis with the intensity values shown as a gray scale. This representation contains the full spectral information and allows later evaluation of excitation as well as emission spectra with an arbitrarily selected bandpass. Note that the interference from O_2 LIF at the Sick excitation is evident in the resolved fluorescence shown in Fig. 2(a). Profiles along the excitation frequency coordinate yields excitation spectra, where the bandpass of the detection can be selected

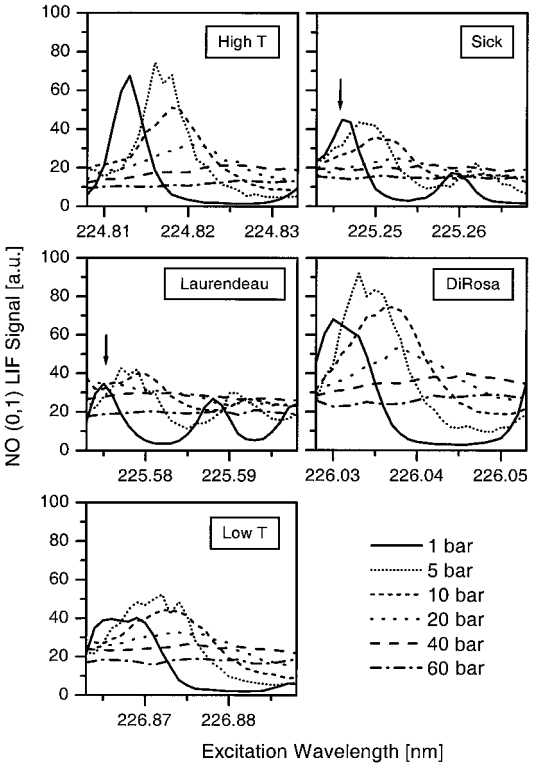

Fig. 3. Fluorescence excitation spectra for the five candidate transitions for the lean $\phi = 0.93$ flames plotted for selected pressures. The arrows indicate the candidate line positions at 1 bar.

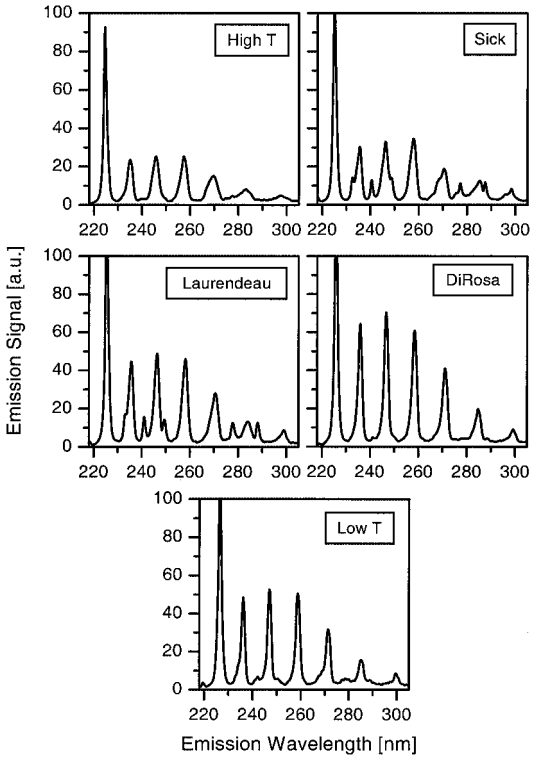

Fig. 4. Fluorescence emission spectra for the five candidate transitions for the p = 40 bar, $\phi = 0.83$ flame. At 225–230 nm, intense Rayleigh scattering adds to the NO (0,0) LIF signal.

arbitrarily over the entire fluorescence range. Similarly, fluorescence spectra can be extracted with the excitation frequency fixed at a given value.

Figure 2(b) gives an example for a two-dimensional spectrum near the Sick transition for $p = 40$ bar and $\phi = 0.83$. Note the difference in the scale of the excitation and emission wavelength axis. The strong emission signal at 225 nm is due to elastically scattered laser light. Emission from the NO A–$X(0,0)$ band also contributes to this signal. The vibrational progression of the NO fluorescence in the A–X band can clearly be seen and is easily distinguished from the vibrational progression of the interference O_2 B–X fluorescence.

A. Excitation Spectra

We extracted fluorescence excitation spectra by plotting the signal in the 4-nm bandpass centered on the wavelength of the maximum of the NO A–$X(0,1)$ emission (236 nm) versus the excitation wavelength. Figure 3 shows spectra around the five candidate transitions for all pressures investigated for the slightly lean ($\phi = 0.93$) flame. The contribution of O_2 LIF to the emission is small in this fluorescence bandpass (see Subsection 5.D).

Collisional line broadening and shifting has been investigated in detail for the NO molecule.[20–22] Its effect can be clearly seen in Fig. 3 as the peak signal shifts to longer excitation wavelengths with pressure. At the same time, line broadening becomes significant and smears out the rotational structure for pressures >10 bar. For all investigated transitions, the peak signal strength increases slightly between 1 and 5 bars and then decreases again for increasing pressure. As we discuss in subsections 5.B–5.D, this variation in signal strength is due to the combined effects of varying excitation efficiency, fluorescence yield, and NO number density. The discussion focuses on comparisons of the different excitation schemes for various flame conditions.

B. Emission Spectra

Fluorescence emission spectra are extracted from the excitation and emission maps as horizontal profiles from the two-dimensional excitation and emission charts. The laser is tuned to the NO LIF peak maximum for each individual pressure for pressures of 1–20 bars. Because of the loss of distinct peaks at higher pressures, the positions of the peaks at 20 bars are also used for the measurements of 40 and 60 bars. Only a limited number of these spectra are shown to demonstrate their typical behavior. Further data reduction leads to the more compact information presented below.

Figure 4 shows emission spectra between 220 and 290 nm for the five candidate transitions in the $p = 40$ bar and $\phi = 0.83$ flame. Dominant features are the Rayleigh signal at the 224–227-nm excitation wavelengths and the NO fluorescence in the A–$X(0,1)$–$(0,5)$ bands at 237, 247, 259, 272, and 285 nm, respectively. The relative intensities of the NO

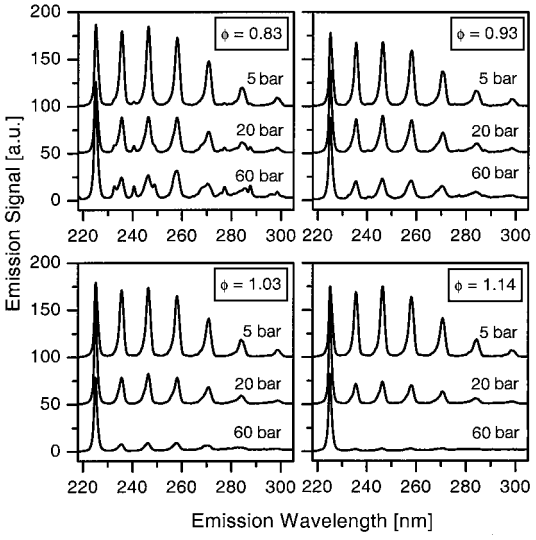

Fig. 5. Fluorescence emission spectra for the Sick transition for the $p = 5$, 20, and 60 bar, $\phi = 0.83$, 0.93, 1.03, and 1.14 flames. At 225–230 nm, intense Rayleigh scattering adds to the NO (0,0) LIF signal.

emissions reflect the Franck–Condon coefficients,[39] convoluted with the collection efficiency of the spectrograph and camera system that has a maximum at approximately 280 nm. Especially for the Sick and the Laurendeau transitions, the vibrational progression of the O_2 fluorescence is also visible. The purity of the NO signal in terms of O_2 interference and the NO signal strength is qualitatively observed from such spectra. The interference and signal strength can be quantitatively compared by use of a multiple Gaussian fitting technique described in Subsection 5. C.

The influence of pressure and the equivalence ratio on the NO and O_2 LIF emissions is shown in Fig. 5 for the Sick transition. Emission spectra are shown for $p = 5$, 20, and 60 bars and equivalence ratios of 0.83, 0.93, 1.03, and 1.14. Relative O_2 LIF interference increases with increasing pressure and decreasing equivalence ratio. It should be mentioned that the O_2 LIF contribution disappears in the rich flames. In the rich flames with increasing pressure, the NO signal disappears faster than in the lean flames. Here, the NO added to the fresh gases is affected by NO reburn reactions. These reactions are known to be much more efficient in rich flames.[40–42]

C. NO Signal Strength

The relative contributions of NO and O_2 LIF were evaluated with a nonlinear least-squares fit of multiple Gaussian line shapes to separate the overlapping NO and O_2 signals. A detection bandpass range from 230 to 253 nm was chosen, which includes the NO A–X(0,1) and (0,2) bands as well as three O_2 B–X bands. This represents the most important bandpass for NO detection for practical applications (imaging as well as pointwise detection) because of the large Franck–Condon factors of the NO (0,1) and

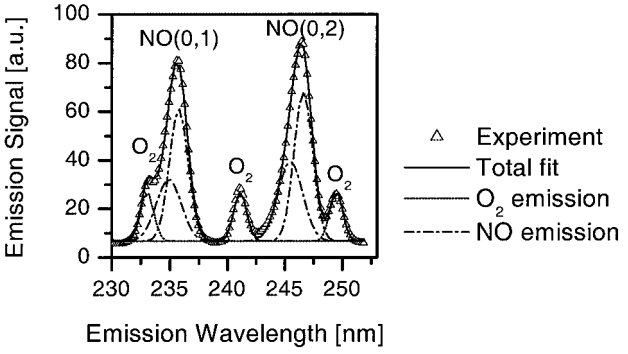

Fig. 6. Example of the nonlinear least-squares fit of seven Gaussians (three for O_2 and four for NO) to the fluorscence spectra between 230 and 253 nm after the Laurendeau transition is excited at $p = 40$ bar, $\phi = 0.83$.

(0,2) bands,[39] which provide strong signals and maximum NO/O_2 LIF ratios. Best-fitting results could be achieved by use of a single Gaussian for each O_2 emission peak (O_2 transitions had sufficiently low rotational quantum numbers) and two Gaussians for each NO emission peak that account for a broader and bimodal NO emission feature.[42] Figure 6 shows the results of the fitting algorithm for the $p = 40$ bar, $\phi = 0.83$ flame with the Laurendeau excitation. NO and O_2 signal strengths are evaluated by integration of the respective Gaussian fits.

The total NO signal strengths in the bandpass region from 230 to 253 nm for the investigated flames are shown in Fig. 7. For a given flame condition (in terms of pressure and equivalence ratio) the absolute NO and O_2 number densities as well as the temperature are identical for all candidates, enabling a direct relative comparison. Figure 7 reveals a large difference in signal strengths for the different candidates. Generally, transitions that consist of multi-

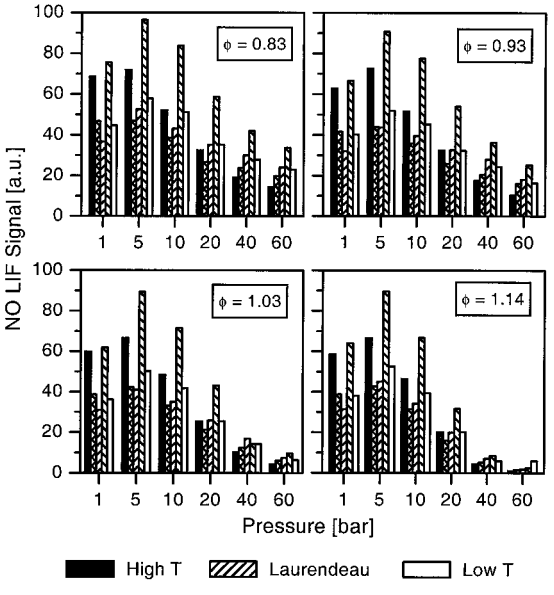

Fig. 7. Total NO fluorescence signal between 230 and 253 nm for the candidate excitation wavelengths.

ple overlapping lines (like the DiRosa, high T, and low T features) give higher signal intensities.

A change in flame conditions also changes temperature, number densities, and NO reburn chemistry, thus affecting NO and O_2 LIF signals. A comparison of signal intensities for different flame conditions as well as a comparison of measured and simulated signal strengths is therefore not possible on the present stage. This will be included in forthcoming research including measurements of absolute NO concentrations and temperatures. Nevertheless, on the basis of calculations[32,41] and experiments,[40] it can be assumed that, in the lean flames, reburn reactions lead to a <10% uncertainty in local NO concentrations.

An optimized strategy for NO detection should involve excitation of the transition at maximum signal strength as a function of pressure. This, however, is not possible in environments with fluctuating pressure (e.g., internal combustion engines). In that case a compromise must be found between signal strength and investigated pressure range. Because of the simultaneous action of pressure broadening and shift, signal variation for a given excitation wavelength is most pronounced for pressures between 1 and 5 bars and much less for higher pressures. For applications with pressures >5 bars we propose using an excitation wavelength at the 5-bar peak. For applications with lower pressure (1–5 bars), the 1-bar peak should be used. This, however, reduces the signal strength at higher pressures.

The pressure influence on NO LIF intensities was simulated on the basis of a four-level model.[43] We calculated NO transition frequencies and rotational line strengths using relations from Paul.[44] Vibrational transition probabilities were taken from Laux and Kruger,[45] and pressure-broadening and pressure-shifting coefficients of NO from DiRosa and Hanson[20] and Vyrodov *et al.*[22] were applied. Calculations were carried out for the laser line width of our system of 0.4 cm^{-1} FWHM and additional line widths of 0.5 and 0.25 cm^{-1}, respectively, typical for the Raman-shifted tunable excimer system and the optical parametric oscillator system.

In Fig. 8 the resulting calculated pressure dependence is shown for the DiRosa and the Sick lines. The upper plots assume the tuning to the NO LIF peak maximum for each pressure. Only for pressures ≤5 bars does the laser linewidth influence the LIF signal; at higher pressures, broadening of the NO transitions becomes dominant. The lower curves show the relative loss in signal when a single laser wavelength is used throughout the whole pressure range. Tuning the laser to the NO LIF maximum at 1 bar leads to an increased pressure sensitivity in the intermediate pressure range (10–40 bars, whereas tuning the laser to the 10-bar maximum leads to signal loss at low pressures (<5 bars). Reduced overall pressure sensitivity is achieved when the laser is tuned to the NO LIF maximum at 5 bars. Figure 8 also shows that pressure variations are more severe with narrow-band lasers. The overlap

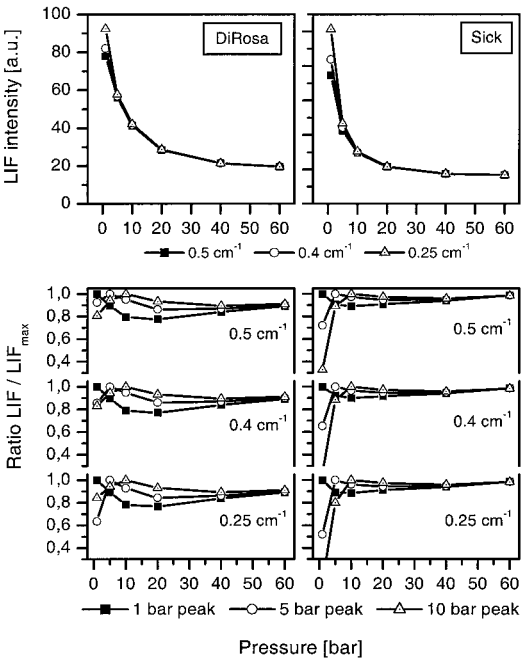

Fig. 8. Calculations of the pressure dependence of the NO LIF signal for T = 2000 K; laser linewidths of 0.25, 0.4, and 0.5 cm^{-1}; and constant NO mole fraction for the DiRosa and Sick transitions. Upper panels: LIF signal for excitation at peak for each individual pressure. Lower panels: loss of NO LIF signal when a constant excitation wavelength is used for a wide pressure range instead of actual pressure-shifted excitation wavelengths optimized for each pressure.

of the multiple lines of the DiRosa transition leads to a broad excitation feature even at low pressures, strongly reducing pressure sensitivity in the p = 1–5-bar range in comparison with the Sick transition.

D. Oxygen Laser-Induced Fluorescence Background

The O_2 LIF background is also assessed from the Gaussian fits. Figure 9 shows the ratio of O_2 emission to the total emission of NO plus O_2 for all five candidate lines. The error bars represent the uncertainties that are due to the fitting algorithm. As discussed qualitatively in Sub section 5.B, O_2 interference generally increases with increasing pressure and decreasing equivalence ratio. The latter is simply an effect of an increasing O_2 number density in the exhaust gases of lean flames. Indeed, for the slightly rich ϕ = 1.03 flame, the O_2 LIF signal is almost not visible (compare with Fig. 5). The data in Fig. 9 are shown for equivalence ratios of ϕ = 0.83 and 0.93. In the ϕ = 1.03 and 1.14 flames as well as for all equivalence ratios at 1 bar, O_2 LIF signals were too weak to measure.

The five candidate transitions were chosen to effectively suppress O_2 interference. Still, from Fig. 9 a surprisingly large difference between the candidates becomes evident. Although excitation of the Laurendeau and Sick transitions leads to strong O_2 interference (up to 29% for the highest pressure and lowest equivalence ratio investigated), excitation of

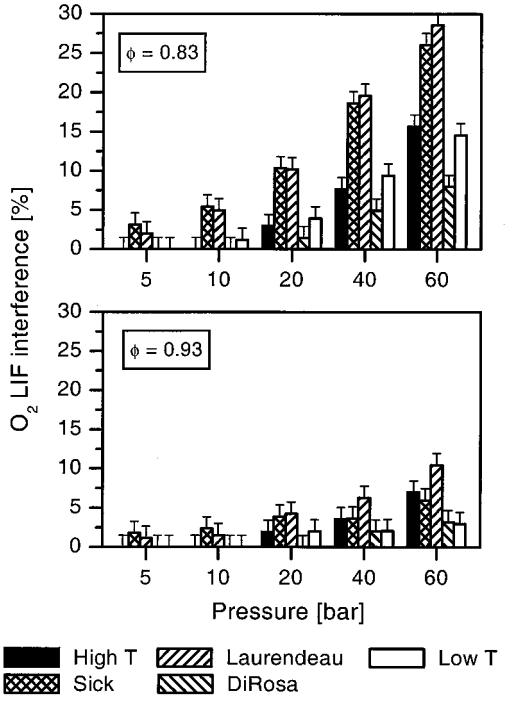

Fig. 9. O_2 LIF contribution to the total NO plus O_2 LIF signal between 230 and 253 nm.

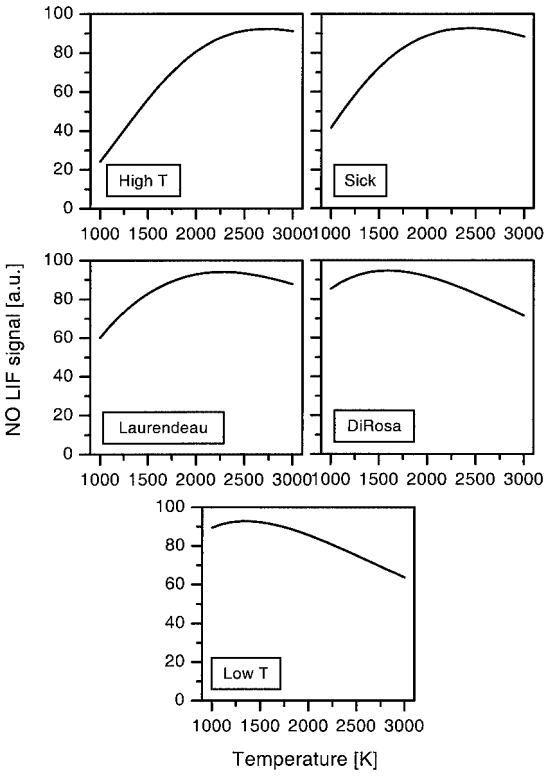

Fig. 10. Temperature dependence of the NO LIF signal for the number density. Stimulation for $p = 10$ bars.

the DiRosa transition under the same conditions reduces the interference to ≤8%. This excellent performance is due to both the high NO signal strength (as discussed in Sub section 5. C) as well as the low O_2 LIF contribution. Note that Bräumer *et al.*[6] could access only a limited range of transitions with their Raman-shifted tunable KrF excimer laser. The high-T transition is an alternative line within the tuning range of that laser system. With an interference of only 16% for the worst-case condition, the high-T transition has a clear advantage over the Sick transition. With ≤15% O_2 LIF interference, the low-T transition provides an intermediate performance.

The present data were evaluated for a rectangular detection bandpass of 242 ± 11 nm. We can further reduce the O_2 LIF interference by applying a narrower detection bandpass, e.g., only around the NO (0,1) or (0,2) emission with 236 ± 5 nm or 247 ± 5 nm, respectively. This leads to further suppression of the O_2 emission around 242 nm. For the $p = 60$ bar, $\phi = 0.83$ flame with Sick excitation, this would reduce the O_2 interference from 26% to 17% or 20%, respectively, and for the Laurendeau excitation from 29% to 21% or 20%, respectively. At the same time the NO signal is reduced by a factor of 0.45 and 0.55 for (0,1) and (0,2) detection, respectively.

Measurements with DiRosa excitation show that O_2 interference stays below 8% and that therefore a background correction is not necessary even for lean ($\phi \geq 0.83$), high-pressure ($p \leq 60$ bars) environments with NO concentrations of approximately 300 parts per million (which is comparable to concentrations present in internal combustion engines.[7]

E. Temperature Sensitivity

Quantitative NO concentration measurements without the exact knowledge of local temperature require one to choose a transition that minimizes the temperature sensitivity. Figures 10 and 11 show that there are significant differences for the five transitions; the main temperature influence comes from the ground-state population of the laser-coupled levels. The respective ground-state energies are listed in Table 1. For practical applications, however, further temperature-dependent effects have to be considered. Because line broadening and shifting is temperature dependent, the overlap of the spectral features with the spectral shape of the laser will also show temperature dependence.

Temperature also influences the fluorescence quantum yield by changing collisional frequencies and quenching cross sections. This influence is identical for all transitions in the same way because the quenching rates do not vary with rotational state for NO. Nevertheless, we included the resulting temperature dependence in the calculations using the Paul *et al.* models for quenching rate coefficients.[17,46] For simplification we make the assumption of complete combustion in a stoichiometric flame; thus only N_2, H_2O, and CO_2 colliders are included in the calculation. This assumption is valid for the present calculations because neither O_2 and CH_4 nor equilibrium OH that is formed from H_2O at elevated temperatures show a variation of quenching cross section with temperature for $T > 1000$ K.[46]

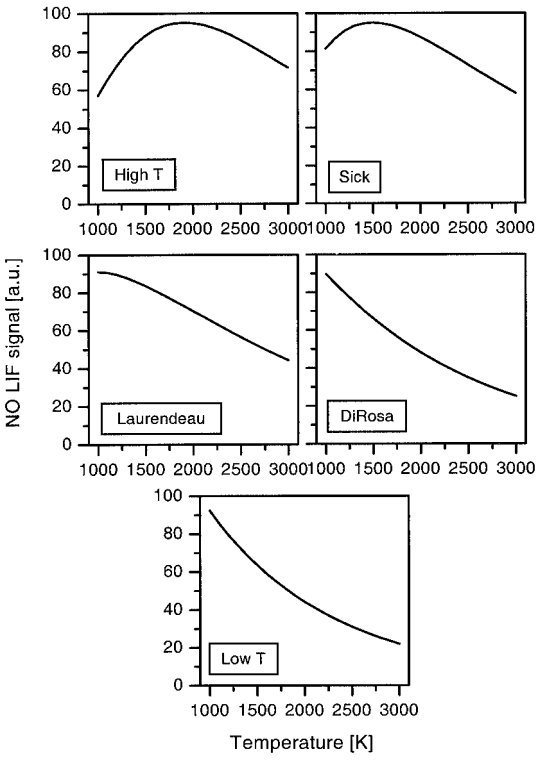

Fig. 11. Temperature dependence of the NO LIF signal for the mole fraction. Simulation for $p = 10$ bar.

We calculated the combined temperature effects of ground-state population, spectral overlap, and quantum yield for the 10-bar flame and the 0.4-cm^{-1} laser FWHM using the model mentioned above in sub section 5. C.[43] Figure 10 shows the temperature sensitivity of LIF intensities for constant NO number densities. The Laurendeau and the DiRosa lines both cover the temperature range relevant for NO measurements in combustion systems (1250–2750 K) with less then ±10% temperature sensitivity. This range for the Sick and the high-T lines is shifted to the 1600 to >3000 K and 1750 to >3000 K region, respectively, and thus these lines can be useful for in-cylinder measurements in internal combustion engines. The low-T line in contrast provides a technique for measuring NO at low temperatures with reduced T sensitivity. This comparison also enables us to propose a strategy for rotational thermometry. A two-line scheme by use of the DiRosa and high-T lines should give high sensitivity at flame temperatures; including the low-T line in a three-line strategy expands the temperature sensitivity range to include room temperature. Temperature imaging measurements based on these transitions are currently under way.

In many combustion situations, not only is the measurement of local NO number densities necessary, but the direct measurement of the mole fractions $x_{NO} = N_{NO}/N_{total}$ is also necessary. Because of the $1/T$ dependence of N_{total}, the resulting temperature dependence of LIF intensities is altered. Typically this reduces the temperature sensitivity of hot transitions in the moderate temperature range and thus enables their use for quantitative measurements without temperature corrections.[7,47] The results of this approach are shown in Fig. 11. The accessible regions with the Laurendeau and DiRosa lines thereby shift to low temperatures, whereas the LIF maxima of the high-T and the Sick lines are shifted to 1800 and 1500 K, respectively; however, their gradients become steeper.

F. Laser and Signal Attenuation

At the short wavelengths used here for NO detection, the transmission in high-pressure combustion environments is restricted. In our measurements near 225 nm, we find that at 60 bars the laser intensity decreases by 37% over the cross section of the flame (6 mm) (see also Fig. 2). This observation agrees well with calculations based on recently obtained absorption cross sections of hot CO_2 and H_2O.[14] For 2000 K these data predict 40% and 4% absorption by CO_2 and H_2O, respectively. Laser attenuation by NO was negligible.

The distribution of CO_2 in exhaust gases is usually reasonably well known. However, because CO_2 absorption cross sections are strongly temperature dependent, additional information on local temperatures would be required for correction of light attenuation. For two-line or multiline temperature measurements, however, the CO_2 absorption causes no additional problems. Because CO_2 absorption cross sections show little dependence on wavelength variations of a few nanometers, local laser intensities can be considered identical for different excitation wavelengths within the A–X(0,0) band. Therefore the effects of CO_2 absorption cancel out when temperatures are calculated from intensity ratios.

6. Summary

LIF measurements were performed for NO A–X(0,0) excitation in laminar, premixed methane and air flames between 1 and 60 bars with equivalence ratios between 0.83 and 1.14. Five different excitation strategies have been investigated and compared for feasibility of quantitative NO diagnostics in high-pressure flames. Of these five, the $P_1(23.5)$, $Q_1 + P_{21}(14.5)$, $Q_2 + R_{12}(20.5)$ (DiRosa) excitation feature at 226.03 nm shows the best performance in terms of minimizing molecular oxygen LIF interference as well as maximizing signal strength. The results show that even for lean ($\phi \geq 0.83$) and high-pressure ($p \leq 60$-bar) environments with NO seeding of approximately 300 parts per minute, O_2 LIF interference is ≤8% for the DiRosa excitation. This transition offers clear advantages over the frequently used $Q_2(26.5)$ (Laurendeau) line at 225.58 nm that has an O_2 LIF interference background as large as 29%.

The limited tuning range of a Raman-shifted tunable KrF excimer laser restricts the set of possible NO excitation transitions. We find here that the newly proposed $R_1 + Q_{21}(26.5)$, $Q_2 + R_{12}(34.5)$, $P_1(40.5)$ (high-T) feature at 224.82 nm significantly reduces

the O_2 LIF interference ($\leq$16% for all investigated flames) in comparison with the previously used $R_1 + Q_{21}(21.5)$ (Sick) transition at 225.25 nm (27% maximum O_2 LIF interference).

We also explored the possible excitation strategies for NO rotational thermometry. Investigations on the $P_2 + Q_{12}(1.5–4.5)$ (low-T) transition at 226.87 nm with a low ground-state energy show an O_2 LIF background of $<$14% for all investigated flames. Together with the DiRosa and the high-T transitions, two- or three-line rotational thermometry should be feasible even in lean high-pressure environments.

Our research at Stanford University was supported by the U.S. Air Force Office of Scientific Research, Aerospace Sciences Directorate, with Julian Tishkoff as the technical monitor. The Division of International Programs at the National Science Foundation supports the Stanford collaboration through a cooperative research grant. The University of Heidelberg research and the travel of W. Bessler and C. Schulz are sponsored by the Deutsche Forschungsgemeinschaft and the Deutsche Akademische Auslandsdienst.

References

1. A. C. Eckbreth, *Laser Diagnostics for Combustion, Temperature, and Species*, 2nd ed. (Gordon and Breach, Amsterdam, The Netherlands, 1996).
2. K. Kohse-Höinghaus, "Laser techniques for the quantitative detection of reactive intermediates in combustion systems," Prog. Energy Combust. Sci. **20,** 203–279 (1994).
3. T. M. Brugmann, G. G. M. Stoffels, N. Dam, W. L. Meerts, and J. J. ter Meulen, "Imaging and post-processing of laser-induced flourescence from NO in a Diesel engine," Appl. Phys. B **64,** 717–724 (1997).
4. C. S. Cooper and N. M. Laurendeau, "Parametric study of NO production via quantitative laser-induced fluorescence in high-pressure, swirl-stabilized spray flames, in *Proceedings of the Combustion Institute* (Combustion Institute, Pittsburgh, Pa., 2000), Vol. 28, pp. 287–293.
5. J. E. Dec and R. E. Canaan, "PLIF imaging of NO formation in a DI Diesel engine," SAE 980147 (Society of Automotive Engineers, Warrendale, Pa., 1998).
6. A. Bräumer, V. Sick, J. Wolfrum, V. Drewes, R. R. Maly, and M. Zahn, "Quantitative two-dimensional measurements of nitric oxide and temperature distributions in a transparent SI engine," SAE 952462 (Society of Automotive Engineers, Warrendale, Pa., 1995).
7. W. G. Bessler, C. Schulz, M. Hartmann, and M. Schenk, "Quantitative in-cylinder NO-LIF imaging in a direct-injected gasoline engine with exhaust gas recirculation," SAE 2001-01-1978 (Society of Automotive Engineers, Warrendale, Pa., 2001).
8. F. Hildenbrand, C. Schulz, J. Wolfrum, F. Keller, and E. Wagner, "Laser diagnostic analysis of NO formation in a direct injection Diesel engine with pump-line nozzle and common-rail injection systems," in *Proceedings of the Combustion Institute* (Combustion Institute, Pittsburgh, Pa., 2000), Vol. 28, pp. 1137–1144.
9. J. M. Seitzman, G. Kychakoff, and R. K. Hanson, "Instantaneous temperature field measurements using planar laser-induced fluorescence," Opt. Lett. **10,** 439–441 (1985).
10. B. K. McMillin, J. L. Palmer, and R. K. Hanson, "Temporally resolved, two-line fluorescence imaging of NO temperature in a transverse jet in a supersonic cross flow," Appl. Opt. **32,** 7532–7545 (1993).
11. W. G. Bessler, F. Hildenbrand, and C. Schulz, "Two-line laser-induced fluorescence imaging of vibrational temperatures of No-seeded flame." Appl. Opt. **40,** 748–756 (2001).
12. J. L. Palmer and R. K. Hanson, "Shock tunnel flow visualization using planar laser-induced fluorescence imaging of NO and OH," Shock Waves **4,** 313–323 (1995).
13. F. Hildenbrand and C. Schulz, "Measurements and simulation of in-cylinder UV-absorption in spark ignition and Diesel engines," Appl. Phys. B **73,** 165–172 (2001).
14. C. Schulz, J. D. Koch, D. F. Davidson, J. B. Jeffries, and R. K. Hanson, "ultraviolet absorption spectra of shock-heated carbon dioxide and water between 900 and 2800 K," Chem. Phys. Lett. **355,** 82–88 (2002).
15. C. Schulz, V. Sick, J. Wolfrum, V. Drewes, M. Zahn, and R. Maly, "Quantitative 2D single-shot imaging of NO concentrations and temperatures in a transparent SI engine," in *Proceedings of the Twenty-Sixth Symposium* (*International*) *on Combustion* (Combustion Institute, Pittsburgh, Pa., (1996), pp. 2597–2604.
16. G. Herzberg, *Spectra of Diatomic Molecules*, Vol. 1 of Molecular Spectra and Molecular Structure (Krieger, Malabar, Fla., 1950).
17. P. H. Paul, J. A. Gray, J. L. Durant, Jr., and J. W. Thoman, Jr., "A model for temperature-dependent collisional quenching of NO $A^2\Sigma^+$," Appl. Phys. B **57,** 249–259 (1993).
18. B. R. Lewis, S. T. Gibson, and P. M. Dooley, "Fine-structure dependence of predissociation linewidth in the Schumann-Runge bands of molecular oxygen," J. Chem. Phys. **100,** 7012–7035 (1994).
19. V. Sick, M. Decker, J. Heinze, and W. Stricker, "Collisional processes in the B state of O_2," Chem. Phys. Lett. **249**, 335–340 (1996).
20. M. D. DiRosa and R. K. Hanson, "Collision-broadening and -shift of NO $\gamma(0,0)$ absorption lines by H_2O, O_2 and NO at 295 K," J. Mol. Spectrosc. **164,** 97–117 (1994).
21. M. D. DiRosa and R. K. Hanson, "Collisional broadening and shift of NO $\gamma(0,0)$ absorption lines by O_2 and H_2O at high temperatures," J. Quant. Spectrosc. Radiat. Transfer **52,** 515–529 (1994).
22. A. O. Vyrodov, J. Heinze, and U. E. Meier, "Collisional broadening of spectral lines in the A-X(0,0) system of NO by N_2, Ar, and He at elevated pressures measured by laser-induced fluorescence," J. Quant. Spectrosc. Radiat. Transfer **53,** 277–287 (1995).
23. F. Hildenbrand, C. Schulz, V. Sick, H. Jander, and H. Gg. Wagner, "Applicability of KrF excimer laser induced fluorescence in sooting high-pressure flames," Deutscher Flammentag, VDI-Gesellschaft Energietechnik-Düsseldorf, VDI Verlag 1492 (1999), pp. 269–274.
24. C. Schulz, V. Sick, J. Heinze, and W. Stricker, "Laser-induced-fluorescence detection of nitric oxide in high-pressure flames with A–X(0,2) excitation," Appl. Opt. **36,** 3227–3232 (1997).
25. A. Brockhinke, A. T. Hartlieb, K. Kohse-Höinghaus, and D. R. Crosley, "Tunable KrF laser-induced fluorescence of C_2 in a sooting flame," Appl. Phys. B **67,** 659–665 (1998).
26. A. O. Vyrodow, J. Heinze, M. Dillmann, U. E. Meier, and W. Stricker, "Laser-induced fluorescence thermometry and concentration measurements on NO A–X (0,0) transitions in the exhaust gas of high pressure CH_4/air flames," Appl. Phys. B **61,** 409–414 (1995).
27. E. J. van den Boom, P. B. Monkhouse, C. M. I. Spaanjaars, W. L. Meerts, N. J. Dam, and J. J. ter Meulen, "Laser diagnostics in a diesel engine," in *ROMOPTO 2000*: *Sixth Conference on Optics*, V. I. Vlad, ed., Proc. SPIE **4430,** 593–606 (2001).
28. B. E. Battles and R. K. Hanson, "Laser-induced fluorescence

measurements of NO and OH mole fraction in fuel-lean, high-pressure (1–10 atm) methane flames: fluorescence modeling and experimental validation," J. Quant. Spectrosc. Radiat. Transfer **54**, 521–537 (1995).
29. M. D. DiRosa, K. G. Klavuhn, and R. K. Hanson, "LIF spectroscopy of NO and O_2 in high-pressure flames," Combust. Sci. Technol. **118,** 257–283 (1996).
30. W. P. Partridge, Jr., M. S. Klassen, D. D. Thomsen, and N. M. Laurendeau, "Experimental assessment of O_2 interferences on laser-induced fluorescence measurements of NO in high-pressure, lean premixed flames by use of narrow-band and broadband detection," Appl. Opt. **34,** 4890–4904 (1995).
31. D. D. Thomsen, F. F. Kuligowski, and N. M. Laurendeau, "Background corrections for laser-induced-fluorescence measurements of nitric oxide in lean, high-pressure, premixed methane flames," Appl. Opt. **36,** 3244–3252 (1997).
32. J. R. Reisel and N. M. Laurendeau, "Quantitative LIF measurements and modeling of nitric oxide in high-pressure $C_2H_4/O_2/N_2$ flames," Combust. Flame **101,** 141–152 (1995).
33. D. Charlston-Goch, B. L. Chadwick, R. J. S. Morrison, A. Campisi, D. D. Thomsen, and N. M. Laurendeau, "Laser-induced fluorescence measurements and modeling of nitric oxide in premixed flames of $CO + H_2 + CH_4$ and air at high pressures," Combust. Flame **125,** 729–743 (2001).
34. T. Dreier, A. Dreizler, and J. Wolfrum, "The application of a Raman-shifted tunable KrF excimer laser for laser-induced fluorescence combustion diagnostics," Appl. Phys. B **55,** 381–387 (1992).
35. I. S. McDermid and J. B. Laudenslager, "Radiative lifetimes and electronic quenching rate constants for single-photon-excited rotational levels of NO($A^2\Sigma^+$, $v' = 0$)," J. Quant. Spectrosc. Radiat. Transfer **27,** 483–492 (1982).
36. W. G. Bessler, C. Schulz, T. Lee, D. Shin (Stanford University), J. B. Jeffries, and R. K. Hanson, are preparing a manuscript to be called "Strategies for laser-induced fluorescence detection of nitric oxide in high-pressure flames. II. A–X(0,1) excitation,"
37. We are preparing a manuscript to be called "Strategies for laser-induced fluorescence detection of nitric oxide in high-pressure flames. III. Comparison of A–X(0,0), (0,1) and (0,2) excitation."
38. H. Eberius, T. Just, T. Kick, G. Höfner, and W. Lutz, "Stabilization of premixed, laminar methane flames in the pressure regime up to 40 bar," in *Proceedings of the Joint Meeting German/Italian Section* (Ravello, Italy, 1989).
39. L. G. Piper and L. M. Cowles, "Einstein coefficients and transition moment variation for the NO ($A^2\Sigma^+ - X^2\Pi$) transition," J. Chem. Phys. **85,** 2419–2422 (1986).
40. J. Warnatz, U. Maas, and R. Dibble, *Combustion* (Springer-Verlag, Berlin, 1996).
41. A. V. Mokhov, H. B. Levinsky, and C. E. van der Meij, "Temperature dependence of laser-induced fluorescence of nitric oxide in laminar premixed atmospheric-pressure flames," Appl. Opt. **36,** 3233–3243 (1997).
42. C. Schulz, V. Sick, U. Meier, J. Heinze, and W. Stricker, "Quantification of NO A–X(0,2) laser-induced fluorescence: investigation of calibration and collisional influences in high-pressure flames," Appl. Opt. **38,** 1434–1443 (1999).
43. V. Sick (Department of Mechanical Engineering, University of Michigan, Ann Arbor, Mich.), W. Bessler, and C. Schulz are preparing a manuscript to be called "NO spectra simulation code."
44. P. H. Paul, "Calculation of transition frequencies and rotational line strengths in the γ-bands of nitric oxide," J. Quant. Spectrosc. Radiat. Tranfer **57,** 581–589 (1997).
45. C. O. Laux and C. H. Kruger, "Arrays of radiative transition probabilities for the N_2 first and second positive, NO beta and gamma, N_2^+ first negative, and O_2 Schumann-Runge band systems," J. Quant. Spectrosc. Radiat. Tranfer **48,** 9–24 (1992).
46. P. H. Paul, C. D. Carter, J. A. Gray, J. L. Durant, Jr., J. W. Thoman, and M. R. Furlanetto, "Correlations for the NO $A^2\Sigma^+$ ($v' = 0$) electronic quenching cross-section," Sandia Rep. SAND94–8237 UC-1423 (Sandia National Laboratory, Livermore, Calif., 1995).
47. F. Hildenbrand, C. Schulz, F. Keller, G. König, and E. Wagner, "Quantitative laser diagnostic studies of the NO distribution in a DI Diesel engine with PLN and CR injection systems," SAE Tech. Paper 2001-01-3500 (Society of Automotive Engineers, Warrendale, Pa., 2001).